Bioorganic & Medicinal Chemistry 19 (2011) 2090–2102

Contents lists available at ScienceDirect

Bioorganic & Medicinal Chemistry

journal homepage: www.elsevier.com/locate/bmc

Structure–activity relationships of flavonoids as inhibitors of breast cancer resistance protein (BCRP)

Anne Pick [a], Henrik Müller [a], Ralf Mayer [b], Britta Haenisch [c], Ilza K. Pajeva [a,d], Mathias Weigt [a], Heinz Bönisch [c], Christa E. Müller [b], Michael Wiese [a,*]

[a] Pharmaceutical Institute, University of Bonn, Pharmaceutical Chemistry II, An der Immenburg 4, 53121 Bonn, Germany
[b] Pharmaceutical Institute, University of Bonn, Pharmaceutical Chemistry I, An der Immenburg 4, 53121 Bonn, Germany
[c] Institute of Pharmacology and Toxicology, University of Bonn, Reuterstr. 2b, 53113 Bonn, Germany
[d] Institute of Biophysics and Biomedical Engineering, Bulgarian Academy of Science, 1113 Sofia, Bulgaria

ARTICLE INFO

Article history:
Received 20 July 2010
Revised 1 December 2010
Accepted 21 December 2010
Available online 30 December 2010

Keywords:
Breast cancer resistance protein
Multidrug resistance
Hoechst 33342 assay
Flavonoids
P-glycoprotein
QSAR
CoMFA
CoMSIA

ABSTRACT

Flavonoids are an interesting group of natural products ubiquitously present in human diet. Their consumption has been associated with various and differing beneficial health effects. However, several flavonoids have been reported to inhibit the breast cancer resistance protein (BCRP) encoded by the ABCG2 gene. Thus, the consumption of flavonoids with high inhibitory activity could change pharmacokinetics and drug levels of drugs that are BCRP substrates. In cancer patients receiving chemotherapy an increased intake of such flavonoids could lead to adverse effects.

We investigated a structurally diverse set of flavonoids, including derivatives with a rare C-methylated structure that were isolated from plants used in traditional medicine. The flavones retusin and ayanin were found to be highly potent inhibitors of BCRP, showing only slightly less potency than Ko143, the most potent ABCG2 inhibitor known so far. The activity data were analyzed by 2D and 3D QSAR analyses and the results revealed the impact of the different substituents at the various positions of the flavonoid core on activity. Additionally, a lateral 2D QSAR analysis of data collected from the literature was performed aiming to derive more general information about the influence of distinct structural features on the inhibitory potency of flavonoids. The comparative QSAR analyses led to a consistent picture of the effects of the different substituents at various positions of the flavone backbone. The following structural features were found to contribute positively to BCRP inhibition: a hydroxyl group in position 5, double bond between position 2 and 3, and a methoxy group in position 3. The exchange of a 3-methoxy group by an OH-group acting also as a hydrogen bond donor, resulted in decrease in activity underlining the potential role of the hydrogen bond acceptor 3-OCH_3 for the interaction with BCRP.

1. Introduction

The development of multidrug resistance (MDR) is a major obstacle to successful chemotherapeutic treatment of cancer patients. Among the different cellular mechanisms causing MDR, the overexpression of ATP-binding cassette (ABC) transporters represents the most common mechanism that leads to decreased effectiveness of anticancer drugs. These ABC-transporters share in common that they use the energy of ATP hydrolysis to actively transport a wide variety of structurally different substrates out of cells against a concentration gradient. The resulting reduced drug level inside the cells is responsible for chemoresistance.

The human genome encodes 48 ABC-transporters. Based on phylogenetic analysis these ABC-transporters have been classified into seven subfamilies.[1] Among these, members of three subfamilies (B, C and G) have been found to be primarily associated with the multidrug resistance phenomenon: ABCB1, P-glycoprotein (P-gp), ABCC1, Multidrug resistance-associated Protein (MRP1), and ABCG2, breast cancer resistance protein (BCRP).[2,3] One common property of the ABC export proteins is that their functional form is comprised of four core units: two transmembrane domains (TMD) which are mostly composed of six membrane spanning helices and two nucleotide-binding domains (NBD).

Besides the pathophysiological role of ABC-transporters in MDR, they play a physiological key role in protecting the body against xenobiotic agents, being widely expressed in excreting organs and physiological barriers as the liver, blood–brain-barrier, placenta and intestine.[4–6] Therefore, ABC-transporters can be considered as essential parts of an immune-like defense system.[7]

BCRP, encoded by the ABCG2 gene, has a molecular weight of 72 kDa and contains 655 amino acids. In accordance to the other

* Corresponding author. Tel.: +49 228 735213; fax: +49 228 737929.
E-mail address: mwiese@uni-bonn.de (M. Wiese).

0968-0896/$ - see front matter © 2010 Elsevier Ltd. All rights reserved.
doi:10.1016/j.bmc.2010.12.043

members of the ABCG subfamily BCRP is a half transporter.[8] Most experimental data indicate that in case of ABCG2 at least homodimerization is necessary for transport function.[7,9]

Since the discovery of BCRP in 1998, the number of identified ABCG2 substrates and inhibitors is increasing continuously. BCRP recognizes a broad variety of positively and negatively charged substances. Prominent substrates of BCRP are the anticancer agents mitoxantrone, flavopiridol, topotecan, SN-38 (the active metabolite of irinotecan), and the tyrosine kinase inhibitors imatinib and gefitinib.[10] Further substrates belonging to other pharmacologic drug classes include folic acid, porphyrin derivatives, HMG-CoA reductase inhibitors (rosuvastatin, pitavastatin, pravastatin and cerivastatin) and many other substances. The first reported BCRP modulator fumitremorgin C (FTC) was isolated from the fermentation broth of *Aspergillus fumigatus*. Due to neurotoxicity, a clinical use of FTC was precluded. Among a series of 42 FTC derivatives the compounds Ko132 and Ko134 have been identified as the most promising candidates. These compounds inhibited BCRP two to three fold more efficiently than FTC with the advantage of significantly lower toxicity.[11,12] Another promising compound from this library is Ko143 which has been shown to lack any toxic effect in mice and to possess even higher potency than Ko132 and Ko134.[13] Due to the weak interaction of these substances with P-gp, they were classified as specific BCRP inhibitors. Novobiocin, a prokaryotic enzyme gyrase inhibitor, has also been reported to specifically interact with BCRP.[14] Some broad-spectrum modulators, for example, tariquidar (XR9576) and elacridar (GF120918), originally developed as 3rd generation P-gp modulators, also interact with BCRP.[15–18] GF120918 was shown to inhibit BCRP function with lower affinity compared to P-gp.[19] Highly active and selective ABCG2 inhibitors derived from XR9576 were recently reported.[20] For tyrosine kinase inhibitors, interactions with BCRP, P-gp and MRP1 were reported.[21] These substances can also be regarded as broad spectrum inhibitors, but may possess an outstanding position due to an additional interaction mechanism via an active PI_3 kinase-actin signaling pathway.[21]

Flavonoids represent another interesting class of BCRP inhibitors. About 6500 naturally occurring flavonoids have been identified up to date.[22] They are important constituents of the human diet, and the daily intake of flavonoids is approximately 200–1000 mg.[23] Major dietary sources of flavonoids include, for example, beverages (cola, red wine, coffee, tea, beer), fruits and fruit juices, vegetables, nuts, potatoes and corn.[24,25] The proposed health optimizing activities are due to the following actions: (i) antioxidant properties through the ability to scavenge reactive species or through their influences on the redox status, (ii) modulation of signal transduction pathways involved in cell proliferation and angiogenesis, (iii) influencing enzymes participating in estrogen biosynthesis, (iv) modulation of enzymes necessary for metabolic activation of procarcinogens and detoxification of carcinogens.[26,27] Additionally, epidemiological and animal studies reveal that the intake of flavonoids potentially decreases the risk of coronary diseases.[28]

Cooray et al. reported that different flavonoids (tested at a final concentration of 30 μM) significantly increased the accumulation of mitoxantrone and bodipy-FL-prazosin in two BCRP overexpressing cell lines.[29] In a study of Zhang et al. twenty naturally occurring flavonoids were investigated with regard to their ability to augment mitoxantrone accumulation in BCRP-positive human breast cancer (MCF-7 MX100) and large cell lung carcinoma (NCI-H460) cells.[30] Among these compounds chrysin and biochanin A were identified as the most promising modulators inhibiting BCRP at concentrations of 0.5–1.0 μM. Ahmed-Belkacem et al. showed that tectochrysin and 6-prenylchrysin exhibited IC_{50} values similar to that of GF120918 in ABCG2-transfected HEK293 cells. A comparison of the inhibitory potencies of twelve different flavonoids indicated that flavones were more efficient than flavonols, isoflavones and flavanones.[31] These findings point to some important aspects: (i) some flavonoids possess rather high inhibitory potencies and may serve as interesting compounds to overcome BCRP-mediated drug resistance in cancer cells. (ii) The pharmacokinetics and drug levels of anticancer agents, which are BCRP substrates might be altered by the intake of flavonoids. An increased consumption of flavonoids as constituents of dietary supplements with proposed health benefits may contribute to significant changes in pharmacokinetics and drug levels of such anticancer agents leading to adverse effects.

The aim of this study was to identify new and potent inhibitors of BCRP among the flavonoids. We investigated 31 flavonoids from different subgroups (flavanones, flavones, flavonols, glycosides, one isoflavone and biflavonoids) for their potential interaction with BCRP. Besides several common flavonoids, compounds present in traditional medicines were also selected. An additional goal was to generate structure–activity relationships based on 2D and 3D QSAR approaches. Lateral 2D QSAR analysis of data collected from the literature was also performed aiming to reveal more information about the influence of distinct structural features on the inhibitory potency of flavonoids.

2. Results

2.1. Characteristics of the investigated cell lines

For a selective investigation of BCRP, it was important to control that MCF-7 MX and MDCK BCRP cells overexpress the ABCG2 gene product BCRP only. Two different approaches were applied: qPCR analysis and labeling of BCRP with the specific antibody 5D3 using flow cytometry detection.[32,33] The results of labeling experiments indicate that MDCK BCRP and MCF-7 MX cells contain high quantities of BCRP in the plasma membrane (Fig. 1a). Concerning MCF-7 MX cells these findings agree with the literature data.[34–37] The MDCK BCRP cell line contains a higher ABCG2 expression level than the MCF-7 MX cell line. The cell lines MCF-7, A2780, A2780adr, MDCK and MDCK MDR1 show no detectable levels of BCRP as the fluorescence intensities were comparable to that of the background fluorescence (Fig. 1a). The results from 5D3 labeling experiments agreed with the findings from qPCR studies indicating at the mRNA and protein expression level that BCRP is clearly overexpressed in MCF-7 MX and MDCK BCRP cells (Fig. 2a).

The expression of P-gp was analyzed using the selective FITC-labeled P-gp antibody MRK-16 with flow cytometry detection.[38,39]

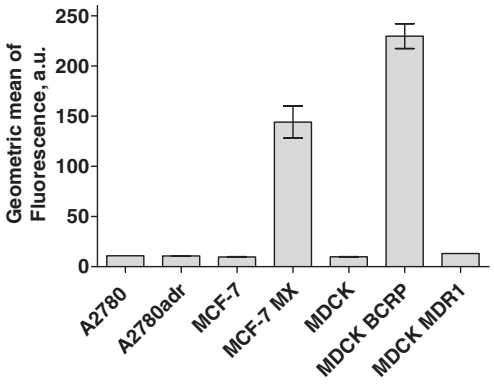

Figure 1a. Expression of BCRP determined with the BCRP specific antibody 5D3 applying flow cytometry detection. Data indicate that BCRP is overexpressed in MCF-7 MX and MDCK BCRP cells only. The other cell lines contain no significant levels of BCRP as fluorescence corresponds to background values (au = arbitrary units).

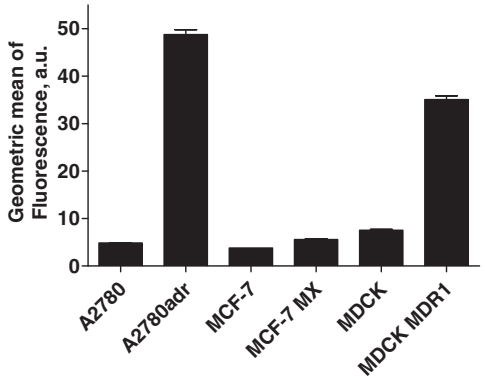

Figure 1b. Expression of P-gp determined with the P-gp specific antibody MRK-16 using flow cytometry detection. Data indicate that P-gp is overexpressed in A2780adr and MDCK MDR1 cells. The other cell lines possess no significant levels of P-gp. MDCK BCRP could not be analyzed by this approach as GFP is excited under these conditions (au = arbitrary units).

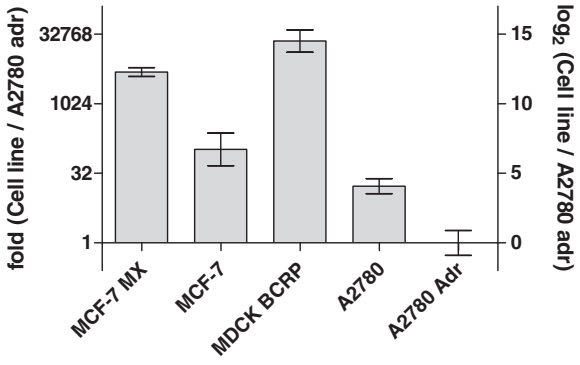

Figure 2a. Relative mRNA expression of ABCG2 in different cell lines determined using sequence-specific primers. No ABCG2 mRNA was detected in MDCK and MDCK MDR1 cells. For the other cell lines mRNA levels are calculated relative to A2780adr, the cell line with the lowest expression of BCRP mRNA, and presented as fold- and $\log_2$-values. Data indicate that ABCG2 mRNA is mostly expressed in MCF-7 MX and MDCK BCRP cells.

Adriamycin resistant A2780adr and MDCK MDR1 cells served as positive controls containing high levels of P-gp as indicated by strong fluorescence intensities (Fig. 1b). In accordance with the results from qPCR experiments (Fig. 2b) labeling studies revealed that A2780adr cells possessed higher P-gp expression levels than MDCK MDR1 cells (Fig. 1b). The results from qPCR experiments proved a very low expression of ABCB1 in the cell lines A2780, MCF-7, MCF-7 MX (Fig. 2b). ABCB1 expression levels in MDCK cells were higher, but still rather low compared to A2780adr and MDCK MDR1 cells. MDCK BCRP cells could not be analyzed with the P-gp specific antibody MRK-16. These cells co-express green fluorescent protein (GFP) which would have been simultaneously excited and therefore would have led to erroneous interpretations.

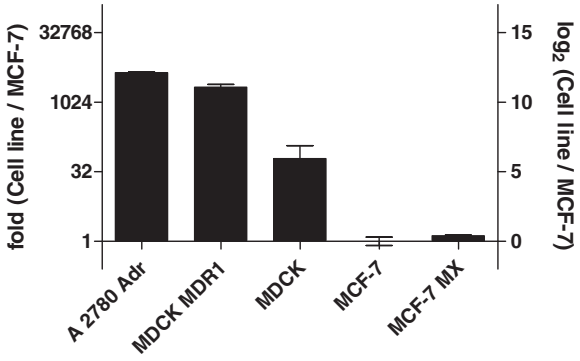

Figure 2b. Relative mRNA expression of ABCB1 in different cell lines determined using sequence-specific primers. No ABCB1 mRNA was detectable in A2780 cells. For the other cell lines mRNA levels are calculated relative to MCF-7, the cell line with the lowest expression of ABCB1 mRNA, and presented as fold- and $\log_2$-values. Data indicate that ABCB1 mRNA is highly overexpressed in A2780adr and MDCK MDR1 cells.

2.2. Inhibition of BCRP by flavonoids

The structures and compound names of the investigated flavonoids are listed in Table 1. The compounds belong to the following major subgroups of flavonoids: flavanones (**1**–**6**), flavones and flavonols (**7**–**23**), glycosides (**24**–**27**), the isoflavone genistein (**28**) and three biflavonoids (**29**–**31**).

To determine the inhibitory potencies of flavonoids against BCRP in MCF-7 MX and MDCK BCRP cells, the Hoechst 33342 assay was applied. It has been previously shown that Hoechst 33342 is a BCRP substrate[5,40,41] and can serve as an effective tool for identification of potential BCRP inhibitors.[18] The inhibitory potencies of the flavonoids obtained in the Hoechst 33342 assay are presented in Table 2. Among the different classes of flavonoids glycosides (**24**–**27**) showed no inhibition of BCRP function. Biflavonoids (**29**–**31**) were found to be poor BCRP inhibitors. Among the investigated flavonoids the flavone derivatives **15** (penduletin), **16** (ayanin) and **17** (retusin) exhibited the lowest IC_{50} values. Retusin (**17**) was only slightly less potent than Ko143 in inhibiting BCRP underlining its high activity. The comparison of the biological activity data of the flavanones **1**, **3** and **5** to their corresponding flavones **8**, **11** and **22** reveals that flavones are stronger inhibitors of BCRP. Figure 3 displays a scatter plot of the pIC_{50} values for the investigated flavonoids obtained in the Hoechst 33342 assay with MCF-7 MX and MDCK BCRP cells, respectively. The high correlation ($R^2 = 0.89$) indicates that BCRP-mediated efflux is the main mechanism of Hoechst 33342 also in MCF-7 MX cells.

Figure 4 illustrates the effects of the 31 flavonoids on the accumulation of calcein AM in P-gp overexpressing A2780adr cells. Remarkably, most of the studied flavonoids investigated at a final concentration of 10 μM showed only very weak inhibition of P-gp function. These results exemplify that the investigated flavonoids possess higher affinity for BCRP than for P-gp.

Among the studied substances, biflavonoids **29**, **30** and **31** exhibited the highest P-gp inhibitory potencies in the calcein AM accumulation assay. For the flavonoids leading to a significant increase in calcein AM accumulation (Fig. 4), complete concentration–response curves were generated. Additionally, their inhibitory effect was determined with flow cytometry detection in MDCK MDR1 cells using rhodamine 123 as a substrate. As expected, the biflavonoids exhibited the lowest IC_{50} values (Table 3). Compound **30** was the most interesting biflavonoid due to its 3–6-fold stronger inhibition of P-gp than verapamil.

In a study of Ahmed-Belkacem et al. the flavonoid 6-prenylchrysin was classified as a specific BCRP inhibitor as almost no interaction with either P-gp or MRP1 was detected.[31] This observation prompted us to investigate the two most effective inhibitors **16** and **17** for their interaction with MRP1 in a calcein AM assay using stably transfected 2008 MRP1 cells. For the standard MRP1 inhibitor indometacin an IC_{50} value of 12.6 ± 6.1 μM was determined in this assay. The inhibition of MRP1 by these flavonoids was almost negligible (IC_{50} >50 μM). Due to the weak inhibition of MRP1 as well as the low inhibitory potency against P-gp, ayanin (**16**) and retusin (**17**) can be classified as rather selective BCRP modulators.

Table 1
Structures and names of the investigated flavonoids

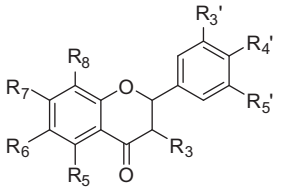

1-6

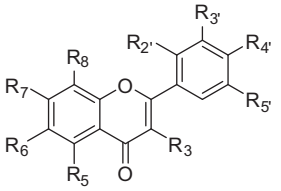

7-23

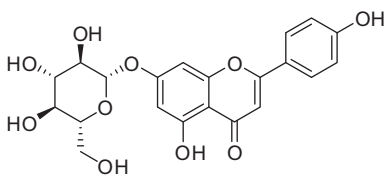

24 (apigetrin)

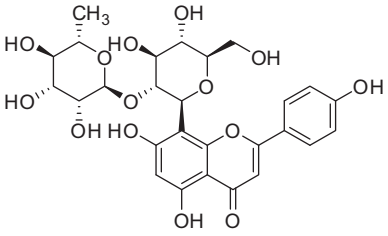

25 (vitexin-2''-O-rhamnosid)

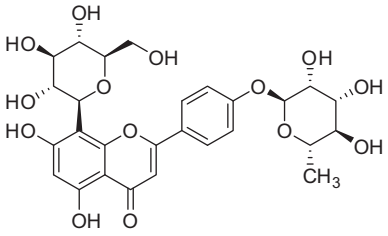

26 (vitexin-4'-rhamnosid)

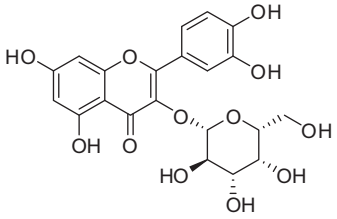

27 (hyperoside)

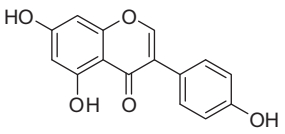

28 (genistein)

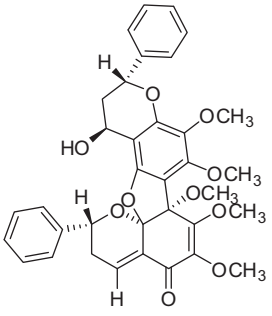

29 (neocalycopteron)

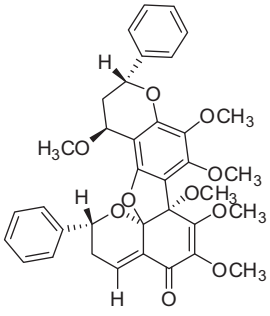

30 (neocalycopteron-4-methylether)

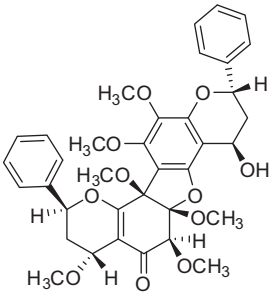

31 (calyflorenon B)

No.	Compound name	R_3	R_5	R_6	R_7	R_8	$R_{2'}$	$R_{3'}$	$R_{4'}$	$R_{5'}$
Flavanones										
1	6-Methoxyflavanon	H	H	OCH_3	H	H	H	H	H	H
2	Pinostrombin	H	OH	H	OCH_3	H	H	H	H	H
3	Dimethylpinocembrin	H	OCH_3	H	OCH_3	H	H	H	H	H
4	Strobopinin	H	OH	CH_3	OH	H	H	H	H	H
5	Strobopinin-7-methylether	H	OH	CH_3	OCH_3	H	H	H	H	H
6	Dimethylcryptostrobin	H	OCH_3	H	OCH_3	CH_3	H	H	H	H

(*continued on next page*)

Table 1 (*continued*)

No.	Compound name	R_3	R_5	R_6	R_7	R_8	$R_{2'}$	$R_{3'}$	$R_{4'}$	$R_{5'}$
Flavones and flavonoles										
7	Flavone	H	H	H	H	H	H	H	H	H
8	6-Methoxyflavone	H	H	OCH_3	H	H	H	H	H	H
9	Apigenin	H	OH	H	OH	H	H	H	OH	H
10	Chrysin	H	OH	H	OH	H	H	H	H	H
11	Chrysin-dimethylether	H	OCH_3	H	OCH_3	H	H	H	H	H
12	Kaempferol	OH	OH	H	OH	H	H	H	OH	H
13	Quercetin	OH	OH	H	OH	H	H	OH	OH	H
14	Morin	OH	OH	H	OH	H	OH	H	OH	H
15	Penduletin	OCH_3	OH	OCH_3	OCH_3	H	H	H	OH	H
16	Ayanin	OCH_3	OH	H	OCH_3	H	H	OH	OCH_3	H
17	Retusin	OCH_3	OH	H	OCH_3	H	H	OCH_3	OCH_3	H
18	Tangeretin	H	OCH_3	OCH_3	OCH_3	OCH_3	H	H	OCH_3	H
19	Sinensetin	H	OCH_3	OCH_3	OCH_3	H	H	OCH_3	OCH_3	H
20	Nobiletin	H	OCH_3	OCH_3	OCH_3	OCH_3	H	OCH_3	OCH_3	H
21	3,5,6,7,8,3′,4′-Heptamethoxy-flavone	OCH_3	OCH_3	OCH_3	OCH_3	OCH_3	H	OCH_3	OCH_3	H
22	5-Hydroxy-6-methyl-7-methoxy-flavone	H	OH	CH_3	OCH_3	H	H	H	H	H
23	Strobochrysin-dimethylether	H	OCH_3	CH_3	OCH_3	H	H	H	H	H
Glycosides										
24	Apigetrin	H	OH	H	O Glucose	H	H	H	OH	H
25	Vitexin-2″-*O*-rhamnoside	H	OH	H	OH	C Sugar	H	H	OH	H
26	Vitexin-4′-rhamnoside	H	OH	H	OH	C Sugar	H	H	O Sugar	H
27	Hyperoside	O Galactose	OH	H	OH	H	H	H	OH	OH
Isoflavone										
28	Genistein	H	OH	H	OH	H	H	H	OH	H

Table 2
Inhibitory potencies of the flavonoids against BCRP expressed in MDCK BCRP and MCF-7 MX cells using the Hoechst 33342 assay

Compound	IC_{50} ± SD (μM)	
	MDCK BCRP	MCF-7 MX
1	19 ± 8	46 ± 16
2	8.9 ± 1.7	31 ± 4
3	17 ± 1	32 ± 5
4	11 ± 4	26 ± 6
5	4.9 ± 1.8	12 ± 2
6	9.3 ± 0.6	17 ± 11
7	17 ± 6	26 ± 8
8	3.4 ± 1.8	10 ± 5
9	3.1 ± 1.0	5.9 ± 1.3
10	1.5 ± 0.3	2.6 ± 1.1
11	9.2 ± 3.0	11 ± 2
12	4.7 ± 1.2	6.2 ± 0.3
13	6.9 ± 1.1	7.6 ± 1.8
14	21 ± 2	49 ± 13
15	1.2 ± 0.6	2.0 ± 1.3
16	0.46 ± 0.04	0.68 ± 0.08
17	0.39 ± 0.14	0.90 ± 0.32
18	19 ± 1	17 ± 5
19	9.0 ± 3.5	8.3 ± 4.3
20	4.9 ± 0.2	4.4 ± 2.7
21	1.4 ± 0.5	1.6 ± 0.9
22	3.0 ± 2.4	2.8 ± 1.7
23	5.9 ± 3.6	8.0 ± 2.3
24	n.i.	n.i.
25	n.i.	n.i.
26	n.i.	n.i.
27	n.i.	n.i.
28	6.9 ± 1.4	8.8 ± 1.3
29	11 ± 2	15 ± 7
30	16 ± 2	47 ± 14
31	29 ± 9	40 ± 2
Ko143	0.21 ± 0.15	0.39 ± 0.01
XR9576	0.94 ± 0.15	1.5 ± 0.1

For comparison, the biological activity data for the standard compounds Ko143 and XR9576 are included. Data shown are means ± SD ($n \geqslant 3$). n.i. = no inhibitory effect detected up to a final concentration of 10 μM.

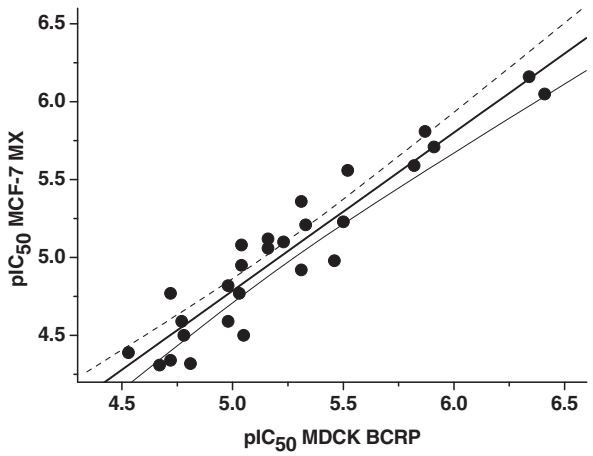

Figure 3. Scatterplot of the pIC_{50} values determined by the Hoechst 33342 assay with MDCK BCRP and MCF-7 MX cells. The squared correlation is 0.87 for all 27 compounds. Each point is an average of at least three independent experiments.

All flavonoids were investigated in A2780 and MCF-7 cells for potential cytotoxicity measuring the amount of ATP within the cells that serves as a sensitive parameter for cell viability.[42] The biflavonoids (**29**–**31**) led to a remarkable decrease of cell viability (Fig. 5) which precludes their use as potential MDR modulators. All other flavonoids had no effect on cell viability at a concentration of 10 μM. Concentration–response curves were generated for the three biflavonoids and Figure 6 exemplary depicts the curve for compound **30**. The IC_{50} values of the three biflavonoids together with the cytostatics cisplatin and doxorubicin, determined for comparison, are given in Table 4.

3. QSAR analyses

So far, only a few studies have been published in which flavonoids were investigated for their BCRP inhibitory potencies. In

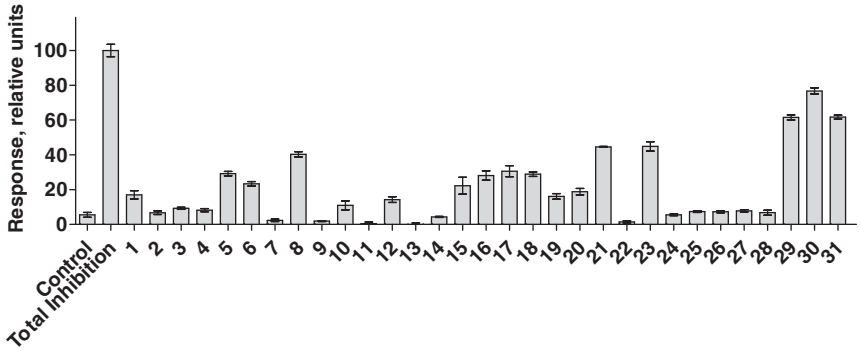

Figure 4. Effects of flavonoids on the accumulation of calcein AM in P-gp overexpresssing A2780adr cells. Flavonoids were investigated at a concentration of 10 μM (n = 3). Data were normalized by defining the inhibition caused by 100 μM verapamil as 100%.

Table 3
Inhibitory potencies of selected flavonoids on P-gp function

Compound	IC_{50} ± SD (μM)	
	A2780adr calcein AM	MDCK MDR1 rhodamine 123
1	39 ± 11	64 ± 17
5	23 ± 11	29 ± 7
6	19 ± 5	15 ± 1
8	13 ± 5	15 ± 6
15	15 ± 2	14 ± 6
16	9.4 ± 1.4	13 ± 5
17	12 ± 2	16 ± 1
18	19 ± 2	39 ± 2
19	34 ± 11	29 ± 9
21	9.0 ± 2.9	31 ± 6
23	8.9 ± 2.1	19 ± 2
29	12 ± 3	8.0 ± 4.7
30	1.7 ± 0.5	1.4 ± 0.4
31	5.6 ± 1.1	8.0 ± 2.2
Verapamil	5.4 ± 2.8	9.8 ± 3.1
XR9576	0.08 ± 0.01	0.21 ± 0.09

The compounds were investigated in the calcein AM and the rhodamine 123 assay using A2780adr and MDCK MDR1 cells. Data shown are means ± SD.

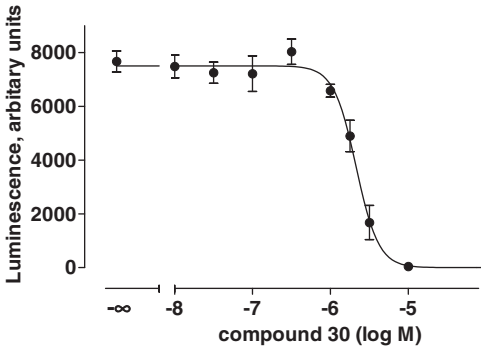

Figure 6. Concentration–response curve of compound **30** obtained in the ATP assay using A2780 cells after a 72 h incubation period (pIC_{50} = 5.67 ± 0.03, n_H = 3.00 ± 0.54). Data shown are averages ± SE from one typical experiment out of a series of three independent experiments.

these studies qualitative structure–activity relationships (SARs) were mostly derived, based on pair wise comparison of the structures and their activity data. A recent review of Nicolle et al. summarizes QSAR and modeling studies of ABCG2-specific inhibitors.[43] and some of them are discussed below in more details. Here we performed 2D and 3D QSAR analyses to describe quantitatively the influence of structural variation on the inhibition of BCRP by the investigated flavonoids. All flavanones and flavones were included, while inactive compounds as well as the structurally different biflavonoids and the singular occurring isoflavone genistein were excluded from the analyses.

3D QSAR analyses applying the CoMFA and CoMSIA methodologies were performed to outline the molecular fields that describe the differences in inhibitory potency. The results of the 3D QSAR analyses using single fields and their combinations are summarized in Table S1. The cross-validated correlation coefficient q^2 serves as a main indicator for the quality of the model.

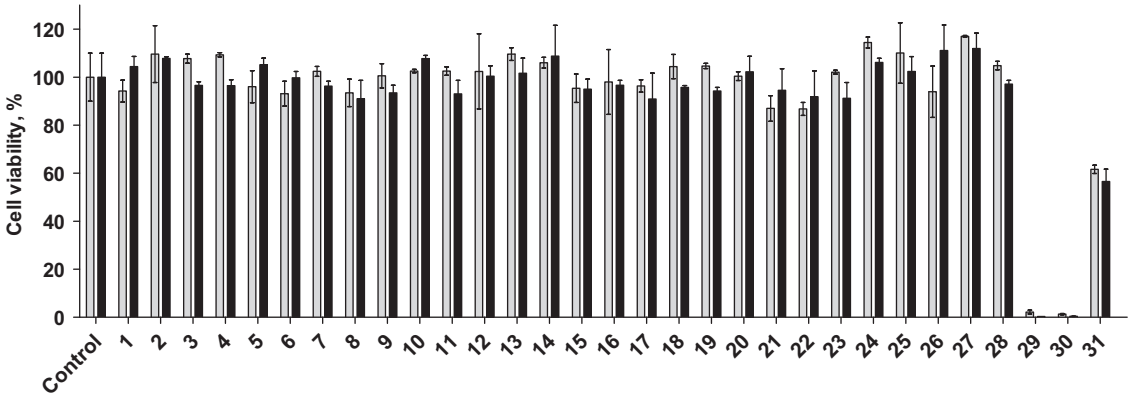

Figure 5. Bar chart illustrating the influence of the studied flavonoids (10 μM) on the cell viability of MCF-7 (grey) and A2780 cells (black).To determine the cell viability the ATP assay was used. Data were normalized by defining the control as 100%.

Table 4
Effects of the biflavonoids **29**, **30**, **31** and of the cytostatic agents cisplatin and doxorubicin on cell viability of A2780 and MCF-7 cells

Compound	IC_{50} ± SD (μM)	
	A2780	MCF-7
29	2.4 ± 0.6	2.4 ± 1.4
30	1.7 ± 0.6	1.9 ± 1.1
31	11 ± 1	15 ± 5
Cisplatin	29 ± 5	27 ± 11
Doxorubicin	0.044 ± 0.018	0.10 ± 0.04

Data were generated using the ATP assay ($n = 3$).

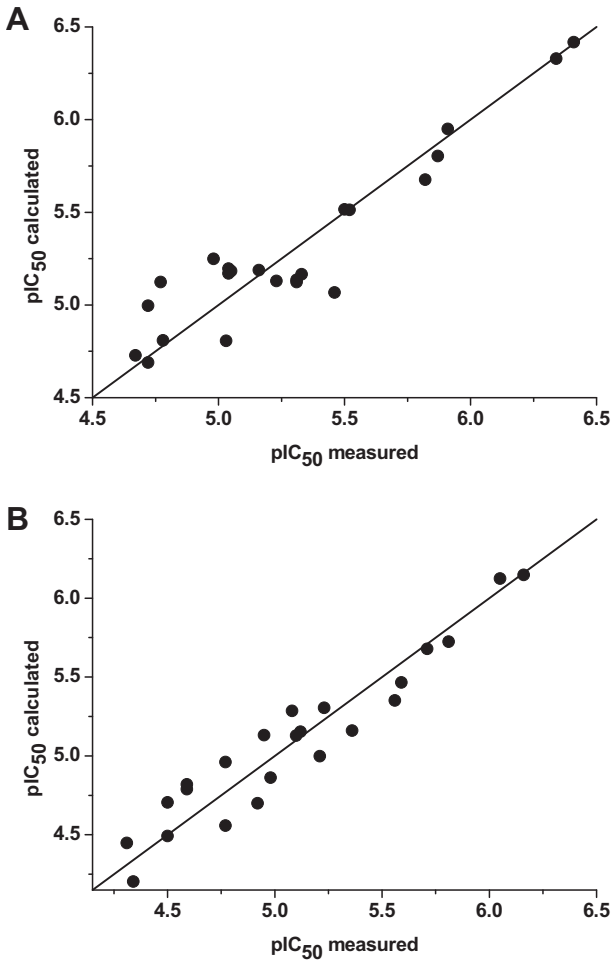

Figure 7. (A) Plot of observed versus calculated potencies for inhibition of BCRP in MDCK BCRP cells. Calculated data were obtained with the CoMSIA model based on the 'ea' fields. (B) The same plot for pIC_{50} values obtained using data from MCF-7MX cells.

In case of CoMFA the hydrogen bonding field alone yielded the best model, and additional inclusion of steric or electrostatic fields led to a small decrease in q^2.

Using the CoMSIA approach the highest q^2 was obtained for the combination of electrostatic and hydrogen bond acceptor field ($q^2 = 0.624$, $n_{opt} = 4$). In Figure 7 the calculated activity data based on the CoMSIA 'ea' model versus the experimental activity data are plotted. As the leave-one-out (LOO) validation may lead to overoptimistic prediction when several compounds with very comparable inhibitory potencies and similar structural properties are present in the dataset, two additional validation techniques were applied to prove that the obtained models were not a result of chance correlation: leave-many-out (LMO) method[44,45] and the scrambling stability test. When performing LMO the dataset was divided into several groups (5/4/3) of equal size and 80–66% of the compounds were included in model generation while the inhibitory potencies of the remaining substances were predicted. As the groups were randomly generated, this procedure was repeated 100 times to exclude the possibility of chance correlations and to validate the models. The results of LMO runs are summarized in Table 5. These results show that the q^2-values decreased moderately, if 33% of the compounds were left out for the model generation. To ensure the validity of the QSAR models a second internal method, the scrambling stability test, was carried out. Under these conditions, the q^2-values have to decrease dramatically to prove that randomly mixed inhibitory potencies are not associated with good predictive power of the models. All averaged q^2-values based on 100 independent random scramblings are negative emphasizing that these models possess no predictive power (Table S2). In summary, results from the internal validation techniques LMO and scrambling stability test point out the validity and robustness of the models.

Contour plots were generated to visualize the contribution of the different substituents to the biological activity of the investigated compounds. Figure 8 depicts the contour plot of the best CoMSIA model with electrostatic and acceptor fields together with the potent compound **16** (ayanin). The red contour of the electrostatic field indicates that a negative charge in this position will lead to increase in the inhibitory potency. In Figure 8 one red contour is localized at the oxygen atom of the methoxy group in position 3 underlining the positive contribution of this structural element to biological activity. This structural element is present in the most potent flavonoids **16** and **17**. A second red contour is seen above the bicyclic ring system of flavones and is due to the electron rich sp^2 hybridized carbon atoms. This red contour illustrates indirectly that flavanones possess a decreased activity compared to flavones. A blue colored area corresponds to the favorable influence of a positive charge to activity, or vice versa shows the unfavorable contribution of a negative charge. One small blue region is falling together with the positive charged hydrogen atom of the hydroxyl group at position 5 of the bicyclic ring system explaining that this structural feature causes an increase of inhibitory potency. The second large blue contour corresponds to the oxygen atom of the 2′-hydroxy group present in the phenyl ring of morin (**14**). This derivative inhibits BCRP with significantly lower potency than its analog kaempferol (**12**) without a 2′-hydroxyl group.

Green and yellow colored regions indicate the positive and negative impact of the hydrogen bond acceptor field. The acceptor field reveals information about where hydrogen bond donating groups on the receptor site enhance anti-BCRP activity. Green contours are localized in position 5 (and 6) and 7 of the benzopyran ring system emphasizing that hydroxy and methoxy groups in this positions increase activity. In position 8 no green contour is present suggesting that methyl and methoxy substituents in this position do not influence the inhibitory potency. The yellow contour reflects the negative impact of a 3-hydroxy group as compared to a corresponding methoxy group.

For the classical QSAR analysis, the Free–Wilson method was applied. This method is especially suitable, when limited structural variety is present at many different substitution positions as given for the investigated flavonoids. When performing the initial Free–Wilson analysis setting the unsubstituted flavone as a reference a multiple collinearity of the descriptors 5-OH, 5-OCH_3, 7-OH and 7-OCH_3 was detected preventing the simultaneous use of all four descriptors. Analysis of the four possible combinations of 3 out of the four descriptors, showed that on omission of either 5-OCH_3, 7-OH or 7-OCH_3 the same set of descriptors remained significant. Thus, the descriptor variable 5-OCH_3 was omitted from the initial

Table 5
Validation of the best 3D QSAR models: results of the leave-many-out validation method; averaged q^2 values and standard deviation (SD) are based on 20 repetitions of the LMO procedure

Number of groups	CoMFA fields		CoMSIA fields	
	e h-bond $q^2 \pm$ SD	h-bond $q^2 \pm$ SD	e a $q^2 \pm$ SD	s e a $q^2 \pm$ SD
MDCK BCRP				
23 (LOO)	0.616	0.619	0.624	0.595
5	0.593 ± 0.089	0.585 ± 0.117	0.601 ± 0.062	0.550 ± 0.097
4	0.554 ± 0.131	0.557 ± 0.167	0.576 ± 0.107	0.528 ± 0.100
3	0.512 ± 0.167	0.503 ± 0.181	0.553 ± 0.101	0.511 ± 0.139
MCF-7 MX				
23 (LOO)	0.605	0.620	0.648	0.625
5	0.589 ± 0.096	0.601 ± 0.099	0.611 ± 0.053	0.600 ± 0.057
4	0.565 ± 0.099	0.567 ± 0.114	0.590 ± 0.065	0.585 ± 0.061
3	0.508 ± 0.140	0.530 ± 0.181	0.520 ± 0.083	0.532 ± 0.066

For comparison, the LOO-values from Table S1 are additionally included.

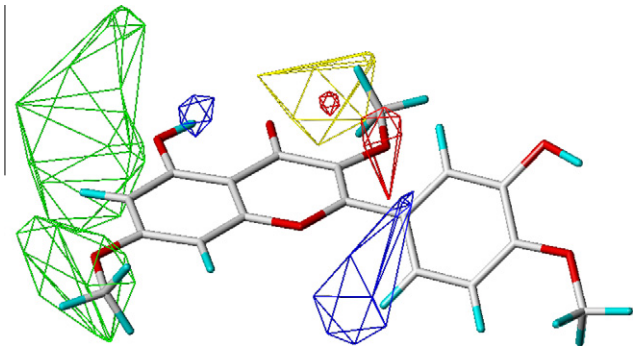

Figure 8. CoMSIA contour plot (STDEV*COEFF) of the 'ea' model for BCRP inhibition using MDCK BCRP cells together with compound **16** (ayanin). Favorable interactions: Green indicates regions of favorable interactions with a hydrogen bond acceptor, yellow indicates unfavorable interactions. Red highlights favorable interactions with a negative charge, while blue indicates regions where a positive charge is favored.

descriptor set. The final models were derived by stepwise elimination of insignificant variables (Eqs. 1 and 2). Depicted are the non-standardized coefficients with 95% confidence intervals given in parenthesis.

$$\begin{aligned} pIC_{50(MX)} = {} & 0.66(\pm 0.25)\ 3\text{-}OCH_3 + 0.43(\pm 0.22)\ 5\text{-}OH \\ & + 0.46(\pm 0.47)\ 8\text{-}CH_3^{*} - 0.71(\pm 0.24)\ \text{flavanon} \\ & - 0.84(\pm 0.46)2'\text{-}OH - 0.30(\pm 0.28)\ 4'\text{-}OH \\ & + 5.03(\pm 0.14) \end{aligned} \quad (1)$$

$^{*}p = 0.053$; $n = 23$, $R^2 = 0.904$, $s = 0.19$, $F = 25.6$.

$$\begin{aligned} pIC_{50(BCRP)} = {} & 0.74(\pm 0.27)\ 3\text{-}OCH_3 + 0.46(\pm 0.23)\ 5\text{-}OH \\ & - 0.38(\pm 0.24)\ \text{flavanon} - 0.62(\pm 0.51)2'\text{-}OH \\ & - 0.29(\pm 0.30)\ 4'\text{-}OH^{*} + 5.12(\pm 0.16) \end{aligned} \quad (2)$$

$^{*}p = 0.057$; $n = 23$, $R^2 = 0.857$, $s = 0.21$, $F = 20.4$.

Repetition of the analyses without compounds **6** and **14** that contain structural elements present only once in the data set led to very similar results with only small changes in the regression coefficients (data not shown). The addition of a methoxy group in position 3 causes a strong increase in BCRP inhibiting potency. Exchanging a hydrogen or methoxy group in position 5 by a hydroxyl group increases BCRP inhibition potency 2–3-fold. The combination of both beneficial substituents in positions 3 and 5 is present in the highly active compounds **16** and **17** (ayanin and retusin).

A significant and remarkable decrease in activity is caused by a hydroxyl group in the 2′-position of the phenyl ring, as present in morin (**14**). Also a 4′-hydroxy group is disadvantageous, while the contribution of a 3′-hydroxy group is highly insignificant.

Aiming to identify general trends in the SARs of flavonoids we also analyzed data reported in the literature. When comparing QSARs derived from data measured in different labs using different assays and cell lines no general correlation is to be expected, but the trends should agree. A substituent that significantly increases activity in one assay, should show a positive, although not necessarily statistically significant, contribution in a related assay. Therefore, we compared in a qualitative way the results obtained from the analysis of our data with the findings emerging from the Free–Wilson analyses of the data collected from the literature. To allow comparison of the contributions of the different substituents, the same reference, flavone, was chosen for the Free–Wilson analyses. In a study of Ahmed-Belkacem et al. 14 flavonoids were investigated using a functional mitoxantrone accumulation assay and ABCG2 transfected HEK293 cells.[31] The data set mainly consisted of chrysin derivatives substituted with different terpenoid groups in position 6 and/or 8. Among the studied flavonoids, many compounds contained single occurring substituents leading to variables with singular values (singularities). Therefore, we performed two analyses: one comprising all variables (Eq. 3) and a second where we excluded singular occurring variables (data not shown). Both analyses led to comparable results.

$$\begin{aligned} pIC_{50(MX\ acc.)} = {} & -0.48(\pm 0.23)\ 3\text{-}OH - 0.32(\pm 0.21)7\text{-}OH \\ & + 1.31(\pm 0.31)\ 6\text{-prenyl} \\ & + 0.77(\pm 0.31)\ 6\text{-geranyl} \\ & + 0.88(\pm 0.31)\ 6\text{-dimethylallyl} \\ & + 0.82(\pm 0.31)\ 8\text{-prenyl} \\ & - 0.32(\pm 0.37)\ 8\text{-geranyl}^{*} \\ & + 0.62(\pm 0.31)\ 8\text{-dimethylallyl} \\ & - 0.44(\pm 0.31)\ 4'\text{-}OH \\ & - 0.36(\pm 0.37)\ \text{flavanon}^{**} + 5.55(\pm 0.17) \end{aligned} \quad (3)$$

$^{*}p = 0.069$, $^{**}p = 0.051$; $n = 14$, $R^2 = 0.996$, $s = 0.08$, $F = 70.1$.

Additionally, three structural features possessed a statistically significant impact on activity: a 4′-OH substituent decreased biological activity, in agreement with the results of the present study. A 3-OH and 7-OH group had also negative impacts on activity.

BCRP inhibition data of a larger number of flavonoids were reported by Zhang et al. in two studies using also mitoxantrone accumulation assay.[30,46] In the earlier study[30] the flavonoids were

investigated at a fixed concentration of 50 μM only in BCRP overexpressing MCF-7 MX100 and NCI-H460 MX20 cells. At this high concentration many of the flavonoids led to almost complete BCRP inhibition with highly enhanced mitoxantrone accumulation that may prevent to derive reliable structure–activity relationships. In the second study IC_{50}-values were determined and reported for a largely overlapping set of 18 flavonoids.[46] Therefore, we analyzed these data using the Free–Wilson approach. The variable 5-OH showed a multiple collinearity with other variables and had to be excluded. The final result is given in Eq. 4.

$$\begin{aligned} pIC_{50(\text{ref. } 46)} = {} & 0.52(\pm 0.39)\ 6\text{-}OCH_3 + 0.34(\pm 0.33) 7\text{-}OH \\ & - 1.31(0.55)\ 8\text{-}OH + 0.54(0.58)\ 8\text{-}CH_3^{*} \\ & - 1.03(\pm 0.26)\ \text{flavanon} - 0.50(\pm 0.35)\ 4'\text{-}OH \\ & + 5.68(\pm 0.28) \end{aligned} \quad (4)$$

$^{*}p = 0.066$; $n = 18$, $R^2 = 0.918$, $s = 0.23$, $F = 20.5$.

A comparison of the effects of the variables in common with our data set showed a general agreement. In the final equation 6-OCH_3, 7-OH and 8-CH_3 contributed positively, while the presence of 4′-OH or flavanon decreased inhibitory activity to an even larger extent as in our assay.

Katayama et al. investigated the reversal effects of 12 flavones and flavanones on BCRP-mediated drug resistance in K562 BCRP cells.[47] The inhibitory potencies of the flavonoids were determined in an indirect way from growth inhibition curves of the anticancer agent SN-38 in absence or presence of a fixed concentration of flavonoids. In contrast to the functional investigations, this methodology presents an indirect approach. The most active compound (**1a** in Ref. 47) was structurally unique, containing a 3-OCH_3 and a 7-OCH_3 group. Additionally, it was more than one order of magnitude more potent than all other flavonoids, therefore it was excluded from the analysis. From Free–Wilson analysis five significant variables were retained, whose contributions are shown in Eq. 5.

$$\begin{aligned} pIC_{50(\text{ref. } 47)} = {} & -0.35(\pm 0.13)\ 3\text{-}OH - 0.48(\pm 0.17)\ \text{flavanon} \\ & - 0.60(\pm 0.13)\ 3'\text{-}OH + 0.16(\pm 0.17)\ 4'\text{-}OH^{*} \\ & + 1.00(\pm 0.19)\ 4'\text{-}OCH_3 + 0.43(\pm 0.15) \end{aligned} \quad (5)$$

$^{*}p = 0.060$; $n = 11$, $R^2 = 0.989$, $s = 0.08$, $F = 93.7$.

A 3-OH-substituent caused reduction of activity, as well as a hydroxyl group in 3′-position of the phenyl ring. Again flavanols were found to be less active, in agreement with the results from ref. 48 and the findings from the present study. However, the coefficients for 4′-hydroxy and especially 4′-methoxy differed, as they were positive and statistically significant in contrast to the results derived from the other analyzed data sets.

The role of lipophilicity as a potentially important parameter for the interaction with BCRP was examined by calculating log P and log $D_{7.4}$ values. With regard to the present study and the literature-based data only poor correlations were found between log P or log $D_{7.4}$ and inhibitory potencies with R^2-values below 0.5 (data not shown). The low q^2 values recorded in our 3D QSAR models employing hydrophobic indices also confirm this observation (Table S1).

We additionally validated our 3D QSAR models using the compounds tested by Zhang et al.[46] as an external data set. Among the several data sets analyzed by us using classical QSAR (Ahmed-Belkacem et al.,[31] Zhang et al.[46] and Katayama et al.,[47] see above), this set appears as the most appropriate one as it has the highest number of compounds tested also in our assays (5 out of 18) and partially overlaps with those in Katayama et al. (7 out of 11).[47] The compounds investigated by Ahmed-Belkacem et al.[31] could not be included in our external set, as they possess large alkyl substituents not present in our structures and thus exceeding the structural space covered by the models.

The plot of the activity data of Zhang et al.[46] versus our activity data of the five overlapping compounds shows a similar general tendency for both, BCRP and MX assays with R^2 of about 0.43 (Supplementary Fig. S1) that is the highest among all external sets analyzed. The other 13 non-overlapping compounds are about equally distributed between the subclasses of flavanones (6 compounds) and flavones (7 compounds) thus allowing a more complete model validation. When judging the test set results, it should be noted that only the ranking can be compared and not the pIC_{50} values themselves as different experimental conditions have been applied.

We predicted the inhibitory effects using several of the best 3D QSAR models derived. As the activity data obtained with both cell lines (MDCK BCRP and MCF-7 MX) are highly intercorrelated (Fig. 3), we show here the results of prediction of all 13 compounds based on the activity data from MCF-7 MX cells only. Figure 9 illustrates the activity values reported by Zhang et al. plotted versus predicted by our CoMFA 'hb' (Fig. 9a) and 'hb + e' (Fig. 9b) models. In both plots the data show similar correlations ($R^2 = 0.63$). Clearly outlined are two clusters of compounds corresponding to the subclasses of flavanones and flavones. While the flavanones are well ranked, in case of flavones two compounds deviate mostly,

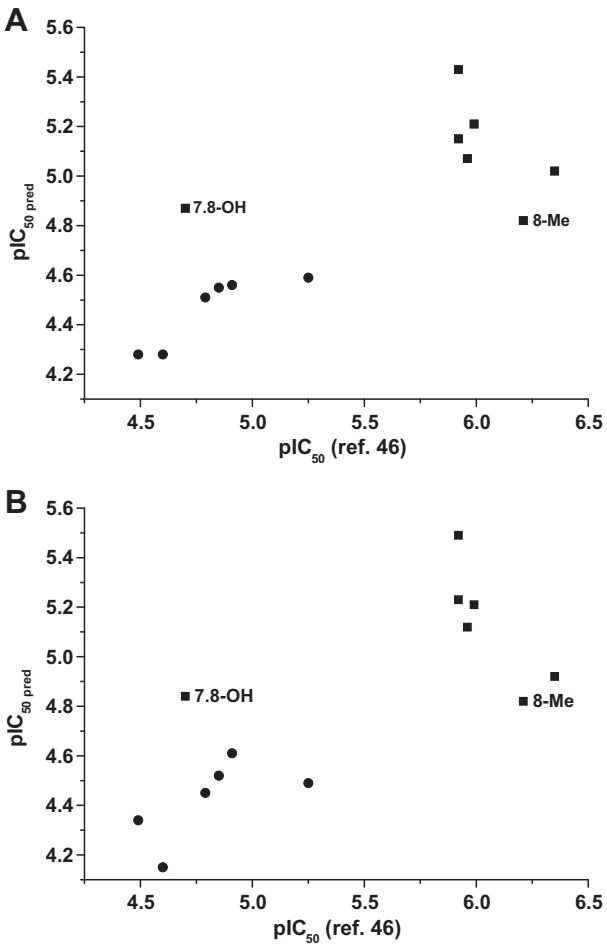

Figure 9. Plots of observed versus predicted activity data for an external test set of 13 flavonoids taken from Zhang et al.[46] Flavanones are indicated by circles and flavones by squares. (A) Based on the CoMFA model using hydrogen bonding and activity data in MCF-7 MX cells. (B) Based on the CoMFA model using combined hydrogen bonding and electrostatic fields and the same activity data.

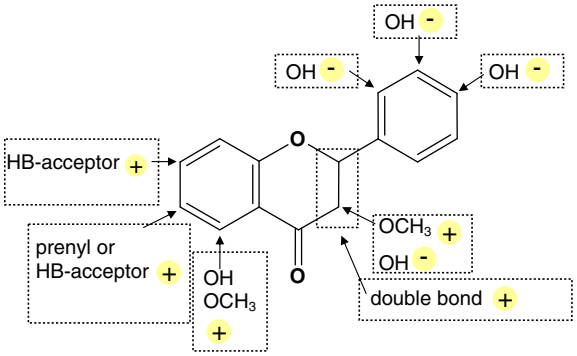

Figure 10. Summary of structural features influencing the inhibition of BCRP by flavonoids. Plus-circles indicate the positive contribution of structural elements to anti-BCRP activity. Minus-circles illustrate the negative impact on inhibitory potency. Results are based on data from the 2D and the 3D QSAR approaches of the present study as well as the findings from 2D analyses of data taken from the literature.

7,8-dihydroxyflavone and 8-methylflavone, and this tendency has been observed in all models validated. It should be noted that in the data of Zhang et al.[46] the activity span for flavones is rather narrow and 7,8-dihydroxyflavone is an exception, having much lower activity. In our set we have no representative with a OH-group at position 8 and this could explain the poor prediction of 7,8-dihydroxyflavone. Moreover, the contour plot (Fig. 8) suggests a negligible role of a substituent in position 8. Interestingly, in the data of Zhang et al. 8-methylflavone has high activity (pIC_{50} = 6.21). Compared to flavone (pIC_{50} = 5.40) introducing a methyl group in position 8 results in 0.8 log unit increase in activity, while in our data the activity increase is only twofold (compare flavanones **3** and **6**).

Including electrostatic fields additionally to hydrogen bond ones achieves better separation between the compounds in both groups, thus confirming the role of this property for the variation in activity of the flavanoids studied (compare Fig. 9A and B).

In general, the validation of the models on an external test set shows a correct ranking of the compounds' activity with similar cross-validated and predicted squared correlation coefficients.

In summary the comparative 2D QSAR analyses and 3D QSAR models validation led to a consistent picture of the effects of the different substituents at various positions of the flavone backbone that is graphically shown in Figure 10.

Figure 10 illustrates the positive contribution of the following structural features to BCRP inhibition: (i) a hydroxyl or methoxy group in position 5, (ii) a double bond between position 2 and 3, (iii) a methoxy group in position 3. Among these structural features the introduction of the methoxy group enhanced the interaction with BCRP most strongly. Compounds sharing all these three structural elements are the most potent inhibitors of BCRP from our flavonoid library. Flavonoids ayanin (**16**) and retusin (**17**) show IC_{50} values which are only slightly higher than that of the most potent BCRP inhibitor Ko143. These substances may serve as lead structures for the design of new effective BCRP modulators. Interestingly, data from the literature as well as the results from the 3D QSAR analysis (Fig. 8) revealed the negative contribution of the hydrogen bond donor, the hydroxyl group localized in position 3, to activity (Eqs. 3 and 5). The presence of the hydrogen bond acceptor 3-OCH_3 plays a crucial role for the interaction with BCRP. The literature data as well as the present study show that a hydroxy group at position 4′ of the phenyl substructure causes a reduction of anti-BCRP activity in functional assays. Again, a transformation into the hydrogen acceptor group OCH_3 may strengthen the interaction with BCRP.

4. Conclusion

Flavonoids have been shown to be associated with a wide variety of anticancer mechanisms. A survival benefit from the intake of flavonoids for cancer patients has been discussed.[28] The bioavailability of flavonoids varies widely and plasma concentrations of approximately 4 μmol/l can be reached.[25] The intestinal concentrations of flavonoids are significantly higher achieving the high micromolar range.[48] A sufficiently high consumption of flavonoids showing strong interaction with BCRP could alter the pharmacokinetics of drugs that are recognized and transported by BCRP including anticancer agents.[27] The influence on pharmacokinetics is due to the expression of BCRP in the apical membrane of enterocytes, the canalicular membrane of hepatocytes, the luminal surface of the brain capillaries and placental synctiotrophoblasts.[1,7] Thus, the knowledge of the interaction of flavonoids with BCRP is important with regard to health benefits, the influence on pharmacokinetics and bioavailability of drugs as well as for the design of flavonoid-type inhibitors of BCRP.

An important goal of the present study was to contribute to understanding of the relationship between structural modifications of flavonoids and their activity. The results from 2D and 3D QSAR analyses enabled to identify the structural features significantly influencing inhibitory potency.

Among the investigated flavonoids the compounds **16** (ayanin) and **17** (retusin) were found to be the most promising BCRP modulators due to their high inhibitory potencies and low toxicities. These modulators belong to the most potent and selective BCRP inhibitors known to date.

5. Experimental

5.1. Chemicals

XR9576 (tariquidar) was a generous gift from Professor Dr. Buschauer (University of Regensburg, Germany). Ko143 was kindly provided by Dr. A. Schinkel (The Netherlands Cancer Institute, Amsterdam, The Netherlands). Doxorubicin was a gift from Medac (Hamburg, Germany). Cisplatin was purchased from Acros (Fairlawn, NJ, USA). All other chemicals were purchased from Sigma Chemicals (Taufkirchen, Germany) unless otherwise stated.

5.2. Sources of flavonoids

Some of the flavanones (**1**, **2**), flavones (**7**–**10**, **12**–**14**) and the flavone glycosides (**24**–**27**) investigated in the present study were purchased (Roth, Karlsruhe, Germany). Ayanin (**16**)[49] and retusin (**17**)[49] were prepared by methylation of commercially available quercetin (**13**) as described previously.[50]

Compounds from natural sources were isolated from two medicinal plants, *Leptospermum scoparium*[52,53] and *Calycopteris floribunda*[54,55] or from an extract of citrus peel (*Citrus reticulata,* polymethoxylated flavones)[51] either.

Preparations of manuka, *Leptospermum scoparium* Forst. (Myrtaceae), the New Zealand tea-tree, are applied in traditional New Zealand medicine against viral infections such as dysenteria, fever and cough. From *Leptospermum scoparium* hybrids, which were cultivated in Germany, some flavanones (**4**, **5**, **6**) and flavones (**22**, **23**) with rare C-methylated backbones were isolated, along with common flavonoids (flavanones **2**, **3**, and the flavone **11**).[52,53]

Calycopteris floribunda Lamk. (Combretaceae) is used as a traditional medicinal plant in some Asian countries. Mainly, it is applied as an anthelmintic and antiviral remedy. *C. floribunda* has also been described to be of use as an antimalarial. However, constituents exhibiting such an activity are still unknown.[54,55]

Peels of citrus fruits (e.g., oranges, tangerines) are natural sources for polymethoxylated flavonoids. Since smaller quantities of these compounds are also present in fruits and juices, they are minor ingredients of daily foodstuffs. Some representatives show remarkable pharmacological activities in diverse enzyme inhibition systems.[51,56]

Four flavones, tangeretin (**18**), sinensetin (**19**), nobiletin (**20**) and heptamethoxyflavone (**21**) were isolated from a tangerine fruit peel extract (*Citrus reticulata* ssp., Rutaceae). The extraction procedure has been previously described.[50]

5.3. Cell culture

The BCRP overexpressing breast cancer cell line MCF-7 MX and the parental cell line MCF-7 were kindly provided by Dr. E. Schneider, Wadsworth Center, Albany, NY, USA.

The cell line MDCK BCRP was a generous gift from Dr. A. Schinkel (The Netherlands Cancer Institute, Amsterdam, The Netherlands). MDCK BCRP cells were generated by transfection of the canine kidney epithelial cell line MDCKII with the human wild-type cDNA C-terminally linked to the cDNA of the green fluorescent protein.[57] The cell line MDCK MDR1 was kindly provided by Dr. P. Borst (The Netherlands Cancer Institute, Amsterdam, Netherlands). The MDCK cell line was purchased from the European collection of animal cell cultures (ECACC; No. 84121903) and was cultivated in DMEM supplemented with 10% fetal bovine serum (FBS) and 50 μl/ml streptomycin, 50 U/ml penicillin. To maintain stable expression of ABCB1 200 μg/ml G-418 was added to the culture medium of MDCK MDR1 cells. Human ovarian carcinoma cell lines A2780 and its corresponding MDR1 overexpressing doxorubicin resistant A2780adr cell line were purchased from ECACC (Nos. 93112519 and 93112520). The cell lines were grown in RPMI-1640 medium supplemented with 10% FBS, 50 μl/ml streptomycin, 50 U/ml penicillin G, and 365 μl/ml L-glutamine.

Cells were grown in a 5% CO_2 humidified atmosphere at 37 °C. Subculturing was performed with 0.05% trypsin and 0.02% EDTA at a confluence of 80–90%. For MCF-7 MX cells every 5th passage mitoxantrone (0.1 μM final concentration) was added to the cell culture medium to conserve ABCG2 overexpression. Before carrying out an experiment, mitoxantrone was removed from the cell suspension and cells were cultivated at least two passages in the absence of the cytostatic drug. MCF-7 MX cells were cultivated for a maximum of 25–30 passages, as then the ABCG2 expression significantly decreased. During the cultivation of MCF-7 MX cells, ABCG2 expression levels were controlled using the BCRP specific 5D3 antibody. To A2780adr cells doxorubicin was added (0.1 μM final concentration) to maintain ABCB1 overexpression. The overexpression of ABCB1 was controlled and confirmed by using the P-gp specific antibody MRK-16. The time interval and preprocessing procedure corresponded to the handling of MCF-7 MX cells, as described above.

5.4. Hoechst 33342 assay

Cell lines were cultivated under standard conditions in T75- or T175-flasks. When reaching a confluence of 80–90%, cells were harvested by gentle trypsination (0.05% trypsin/0.02% EDTA) and then carried over to a 50 ml tube followed by a centrifugation step (266 g, 4 °C, 4 min). Subsequently, the cell pellet was resuspended in fresh culture medium and the cell density was determined using a Casy I Modell TT cell counter device (Schaerfe System GmbH, Reutlingen, Germany). Followed by another centrifugation cells were washed three times with Krebs-Hepes buffer (KHB) and seeded into black 96 well plates (Greiner, Frickenhausen, Germany) at a density of approximately 20,000 cells per well in a volume of 90 μl when using MCF-7 MX or MDCK BCRP cells. The non-BCRP overexpressing counter parts of these both cell lines MCF-7 and MDCK were used as controls to identify unspecific interactions of the investigated substances which could influence the detected fluorescence intensities. For the determination of the inhibitory potencies of substances interacting with P-gp A2780adr cells were seeded into black 96 well plates at a density of approximately 30,000 cells per well in a volume of 90 μl. Ten microliters of various test compounds in different concentrations were added to a total volume of 100 μl. The prepared 96 well plate was kept under 5% CO_2 and 37 °C for 30 min. After this preincubation period, 20 μl of a 30 μM Hoechst 33342 solution (protected from light) was added to each well.

Fluorescence was measured immediately in constant intervals (120 s) up to 2400 s at an excitation wavelength of 355 nm and an emission wavelength of 460 nm applying a 37 °C tempered BMG POLARstar microplate reader (BMG LABTECH, Offenburg, Germany).

5.5. Assay data analyses

The initial, quasi-linear parts of the fluorescence-time curves of Hoechst 33342 were analyzed by linear regression analysis; the slopes were plotted against the corresponding logarithmic concentrations of the investigated compounds. From these data, concentration–response curves were generated by nonlinear regression using the 4-parameter logistic equation with variable Hill slope (GraphPad Prism 5.01 software, San Diego, CA). For normalization of data, slopes from fluorescence–time curves were transformed to relative units by subtracting the lowest determined single value from all other data and thus setting it to zero. The highest measured single value was defined as 100% and all other data were normalized in that range.

5.6. BCRP surface expression

For determining ABCG2 expression the 5D3 primary antibody (Millipore Corporation, Billerica, MA, USA) was used. The experimental procedure was performed according to the manufacturer's protocol. Binding was determined at 488 nm excitation and 585/42 nm emission (FL2) wavelengths applying a flow cytometer (FACS Calibur, Becton Dickinson, Heidelberg, Germany). The samples were measured until 10,000 events were counted or for 20 s. Cell debris or dead cells were eliminated by gating on forward versus side scatter. Data were quantified using the Cell Quest Pro software. At least three independent experiments were performed. The geometric means of the fluorescence were used to calculate the ABCG2 expression status.

5.7. P-glycoprotein surface expression

To investigate P-gp surface expression levels, the FITC labeled monoclonal anti-human P-gp antibody (BD Biosciences, USA) was used following the manufacturer's protocol. Cell counting and data analysis were performed as described for BCRP surface expression except that the band pass filter for FITC (FL1) was used for fluorescence detection.

5.8. qPCR

qPCR was essentially carried out as described previously.[58] Primer sequences used were: 5′-TCCATCATGAAGTGTGACGT-3′ and 5′-GAGCAATGATCTTGATCTTCAT-3′ sense and antisense primers for β-actin, 5′-TGGTACAAGATGATGTTGTGATGG-3′ and 5′-AGATGG AAGGATCAGTGATAAGC-3′ sense and antisense primers for BCRP and 5′-CATTGCTGAGAACATTGCCTATGG-3′ and 5′-CTTTCTGTATCC

AGAGCTGACG-3′ sense and antisense primers for P-gp. Each assay included negative controls (no-template controls) and a standard curve for each gene. The identity of the PCR products was confirmed by melting point analysis after each real-time reaction and then by agarose gel electrophoresis and by dideoxy chain termination sequencing.

Relative mRNA expression was calculated from the ratio cell line/A2780adr for BCRP and from the ratio cell line/MCF-7 for P-gp according to Pfaffl.[59] Thus, relative mRNA expression of the targets was determined related to the cell line with the lowest expression of BCRP and P-gp, respectively. The result for each target gene was normalized by means of the result of the housekeeping gene β-actin and displayed as fold- and $\log_2$-values.

5.9. Determination of cytotoxicity of flavonoids to MCF-7 and A2780 cells using the ATP assay

Cells were seeded into white 96 well plates at a density of 10,000 cells per well in a fixed volume of 90 µl and kept under 5% CO_2 at 37 °C for 4 h. After 4 h, cells were attached and were treated with 10 µl of the different test compounds resulting in a final volume of 100 µl per well. The wells localized on the edges of the 96 well plate were filled only with 100 µl culture medium, but were not used as evaporation effects could influence cell viability. After 72 h incubation, cells were lysed with 1% Triton X100 (final concentration). After 15 min. ATP was determined using a bioluminescence based commercial ATP determination kit (Molecular Probes, Eugene, OR, USA) according to the manufacturer's instructions. Reaction buffer containing dithiothreitol, D-luciferin, and luciferase was injected by using the injector of a Fluostar optima microplate reader (BMG Labtechnologies, Offenburg, Germany). Luminescence was subsequently recorded for 15 s in 0.1 s time intervals.

5.10. Log *P* and log *D* calculations and Free–Wilson-analyses

To calculate the log *P* and log *D* values of the compounds the program ACD log *D*, version 5.09[60] was applied. The multiple linear regression analysis for the Free–Wilson 2D QSARs was performed with SPSS version 14.0 for windows.[61]

5.11. CoMFA and CoMSIA specifications

The CoMFA and CoMSIA calculations were performed with SYBYL.[62] In the CoMFA calculations the following standard settings were used: 2 Å regular grid size in all three directions within an automatically created grid box with 4 Å extension beyond the van der Waals volume of the overlaid molecules, a sp^3 carbon probe with +1 charge, and a distance dependent $(1/r)$ dielectric constant. The following fields were calculated in CoMFA: steric (s), electrostatic (e), and hydrogen bond (h-bnd). The AM1 point charges were applied for calculation of the electrostatic fields. The standard energetic cutoff value of 30 kcal/mol with no electrostatic interactions at bad steric contacts was used. The threshold column filtering was set to 1.0 kcal/mol in all cases. In CoMSIA the following similarity indices fields were calculated: steric (s), electrostatic (e), hydrophobic (h), hydrogen bond donor (d), and hydrogen bond acceptor (a) with the default attenuation factor of 0.3 in the same grid box as used for CoMFA. A common probe atom with 1 Å radius and charge, hydrophobicity and hydrogen bond property of +1 was used. The indices were evaluated according to the usual CoMSIA protocol with 1.0 column filtering. The CoMFA and CoMSIA QSAR equations were calculated by the partial least squares (PLS) method. The internal predictive power of the models was evaluated by leave-one-out (LOO) cross-validation using the cross-validated correlation coefficient q^2, the optimal number of components n, and standard error of prediction SDEP. The linear regression fit was quantified by the squared correlation coefficient r^2 and the standard error of estimates.

Internal validation of the best 3D QSAR models marked in bold in Table S1 was performed by applying the leave-many-out technique (results shown in Table 5). The whole data set was randomly divided into several groups (5/4/3) and the activity of the left-out compounds was predicted. This operation was repeated 100 times to exclude the possibility of chance correlations. The averaged squared cross-validated correlation coefficient and its standard deviation were calculated.

Acknowledgments

The authors thank Dr. A. H. Schinkel (The Netherlands Cancer Institute, Amsterdam, The Netherlands) for kindly providing Ko143 and the MDCK BCRP cell line[40]; Dr. Armin Buschauer, Institute of Pharmaceutical Chemistry, University of Regensburg, Germany, for providing tariquidar; Lisa Gestermann and Annette Glahn for skilfull technical assistance. I.P. acknowledges the support of the National Science Fund of Bulgaria (Grant DTK 02-58). The work has been supported by DFG (Deutsche Forschungsgemeinschaft) Grant GRK677.

Supplementary data

Supplementary data associated with this article can be found, in the online version, at doi:10.1016/j.bmc.2010.12.043.

References

1. Sarkadi, B.; Ozvegy-Laczka, C.; Nemet, K.; Varadi, A. *FEBS Lett.* **2004**, *567*, 116–120.
2. Fojo, T.; Bates, S. *Oncogene* **2003**, *22*, 7512–7523.
3. Bodo, A.; Bakos, E.; Szeri, F.; Varadi, A.; Sarkadi, B. *Toxicol. Lett.* **2003**, *140*, 133–143.
4. Borst, P.; Evers, R.; Kool, M.; Wijnholds, J. *J. Natl. Cancer Inst.* **2000**, *92*, 1295–1302.
5. Doyle, L. A.; Ross, D. D. *Oncogene* **2003**, *22*, 7340–7358.
6. Rao, V. V.; Dahlheimer, J. L.; Bardgett, M. E.; Snyder, A. Z.; Finch, R. A.; Sartorelli, A. C.; Piwnica-Worms, D. *Proc. Natl. Acad. Sci. U.S.A.* **1999**, *96*, 3900–3905.
7. Sarkadi, B.; Homolya, L.; Szakacs, G.; Varadi, A. *Physiol. Rev.* **2006**, *86*, 1179–1236.
8. Shukla, S.; Wu, C. P.; Ambudkar, S. V. *Expert Opin. Drug Metab. Toxicol.* **2008**, *4*, 205–223.
9. Robey, R. W.; Polgar, O.; Deeken, J.; To, K. W.; Bates, S. E. *Cancer Metastasis Rev.* **2007**, *26*, 39–57.
10. Sharom, F. J. *Pharmacogenomics* **2008**, *9*, 105–127.
11. van Loevezijn, A.; Allen, J. D.; Schinkel, A. H.; Koomen, G. J. *Bioorg. Med. Chem. Lett.* **2001**, *11*, 29–32.
12. Allen, J. D.; Schinkel, A. H. *Mol. Cancer Ther.* **2002**, *1*, 427–434.
13. Allen, J. D.; van Loevezijn, A.; Lakhai, J. M.; van der Valk, M.; van Tellingen, O.; Reid, G.; Schellens, J. H. M.; Koomen, G. J.; Schinkel, A. H. *Mol. Cancer Ther.* **2002**, *1*, 417–425.
14. Shiozawa, K.; Oka, M.; Soda, H.; Yoshikawa, M.; Ikegami, Y.; Tsurutani, J.; Nakatomi, K.; Nakamura, Y.; Doi, S.; Kitazaki, T.; Mizuta, Y.; Murase, K.; Yoshida, H.; Ross, D. D.; Kohno, S. *Int. J. Cancer* **2004**, *108*, 146–151.
15. Henrich, C. J.; Bokesch, H. R.; Dean, M.; Bates, S. E.; Robey, R. W.; Goncharova, E. I.; Wilson, J. A.; McMahon, J. B. *J. Biomol. Screening* **2006**, *11*, 176–183.
16. Robey, R. W.; Steadman, K.; Polgar, O.; Morisaki, K.; Blayney, M.; Mistry, P.; Bates, S. E. *Cancer Res.* **2004**, *64*, 1242–1246.
17. Maliepaard, M.; van Gastelen, M. A.; Tohgo, A.; Hausheer, F. H.; van Waardenburg, R. C. A. M.; de Jong, L. A.; Pluim, D.; Beijnen, J. H.; Schellens, J. H. M. *Clin. Cancer Res.* **2001**, *7*, 935–941.
18. Pick, A.; Mueller, H.; Wiese, M. *Bioorg. Med. Chem.* **2008**, *16*, 8224–8236.
19. de Bruin, M.; Miyake, K.; Litman, T.; Robey, R.; Bates, S. E. *Cancer Lett.* **1999**, *146*, 117–126.
20. Kuhnle, M.; Egger, M.; Muller, C.; Mahringer, A.; Bernhardt, G.; Fricker, G.; Konig, B.; Buschauer, A. *J. Med. Chem.* **2009**, *52*, 1190.
21. Lemos, C.; Jansen, G.; Peters, G. J. *Br. J. Cancer* **2008**, *98*, 857–862.
22. Teillet, F.; Boumendjel, A.; Boutonnat, J.; Ronot, X. *Med. Res. Rev.* **2008**, *28*, 715–745.
23. Kuhnau, J. *World Rev. Nutr. Diet.* **1976**, *24*, 117–191.
24. Spencer, J. P. *Proc. Nutr. Soc.* **2008**, *67*, 238–252.
25. Manach, C.; Williamson, G.; Morand, C.; Scalbert, A.; Remesy, C. *Am. J. Clin. Nutr.* **2005**, *81*, 230S–242S.
26. Havsteen, B. H. *Pharmacol. Ther.* **2002**, *96*, 67–202.

27. Wang, M. *Toxicol. Sci.* **2007**, *96*, 203–205.
28. Kohno, H.; Tanaka, T.; Kawabata, K.; Hirose, Y.; Sugie, S.; Tsuda, H.; Mori, H. *Int. J. Cancer* **2002**, *101*, 461–468.
29. Cooray, H. C.; Janvilisri, T.; van Veen, H. W.; Hladky, S. B.; Barrand, M. A. *Biochem. Biophys. Res. Commun.* **2004**, *317*, 269–275.
30. Zhang, S.; Yang, X.; Morris, M. E. *Mol. Pharmacol.* **2004**, *65*, 1208–1216.
31. Ahmed-Belkacem, A.; Pozza, A.; Munoz-Martinez, F.; Bates, S. E.; Castanys, S.; Gamarro, F.; Di Pietro, A.; Perez-Victoria, J. M. *Cancer Res.* **2005**, *65*, 4852–4860.
32. Ozvegy-Laczka, C.; Varady, G.; Koblos, G.; Ujhelly, O.; Cervenak, J.; Schuetz, J. D.; Sorrentino, B. P.; Koomen, G. J.; Varadi, A.; Nemet, K.; Sarkadi, B. *J. Biol. Chem.* **2005**, *280*, 4219–4227.
33. Ozvegy-Laczka, C.; Laczko, R.; Hegedus, C.; Litman, T.; Varady, G.; Goda, K.; Hegedus, T.; Dokholyan, N. V.; Sorrentino, B. P.; Varadi, A.; Sarkadi, B. *J. Biol. Chem.* **2008**, *283*, 26059–26070.
34. van Hattum, A. H.; Hoogsteen, I. J.; Schluper, H. M. M.; Maliepaard, M.; Scheffer, G. L.; Scheper, R. J.; Kohlhagen, G.; Pommier, Y.; Pinedo, H. M.; Boven, E. *Br. J. Cancer* **2002**, *87*, 665–672.
35. van Hattum, A. H.; Schluper, H. M. M.; Hausheer, F. H.; Pinedo, H. M.; Boven, E. *Int. J. Cancer* **2002**, *100*, 22–29.
36. Volk, E. L.; Farley, K. M.; Wu, Y.; Li, F.; Robey, R. W.; Schneider, E. *Cancer Res.* **2002**, *62*, 5035–5040.
37. Volk, E. L.; Rohde, K.; Rhee, M.; McGuire, J. J.; Doyle, L. A.; Ross, D. D.; Schneider, E. *Cancer Res.* **2000**, *60*, 3514–3521.
38. Okochi, E.; Iwahashi, T.; Tsuruo, T. *Leukemia* **1997**, *11*, 1119–1123.
39. Aihara, M.; Aihara, Y.; Schmidtwolf, G.; Schmidtwolf, I.; Sikic, B. I.; Blume, K. G.; Chao, N. J. *Blood* **1991**, *77*, 2079–2084.
40. Clark, R.; Kerr, I. D.; Callaghan, R. *Br. J. Pharmacol.* **2006**, *149*, 506–515.
41. Ifergan, I.; Shafran, A.; Jansen, G.; Hooijberg, J. H.; Scheffer, G. L.; Assaraf, Y. G. F. *J. Biol. Chem.* **2004**, *279*, 25527–25534.
42. Mueller, H.; Kassack, M. U.; Wiese, M. *J. Biomol. Screen.* **2004**, *9*, 506–515.
43. Nicolle, E.; Boumendjel, A.; Macalou, S.; Genoux, E.; Ahmed-Belkacem, A.; Carrupt, P.-A.; Di Pietro, A. *Adv. Drug Deliv. Rev.* **2009**, *61*, 34–46.
44. Tropsha, A.; Gramatica, P.; Gombar, V. K. *QSAR Comb. Sci.* **2003**, *22*, 69–77.
45. Höltje, H.-D.; Sippl, W.; Rognan, D.; Folkers, G. *Molecular Modeling. Basic Principles and Applications*, 3rd ed.; Wiley-VCH: Weinheim, 2008. pp 9–91.
46. Zhang, S.; Yang, X.; Coburn, R. A.; Morris, M. E. *Biochem. Pharmacol.* **2005**, *70*, 627–639.
47. Katayama, K.; Masuyama, K.; Yoshioka, S.; Hasegawa, H.; Mitsuhashi, J.; Sugimoto, Y. *Cancer Chemother. Pharmacol.* **2007**, *60*, 789–797.
48. Scalbert, A.; Williamson, G. *J. Nutr.* **2000**, *130*, 2073S–2085S.
49. Malan, E.; Roux, D. G. *J. Chem. Soc., Perkin Trans. 1* **1979**, 2696–2703.
50. Kaulich, M.; Streicher, F.; Mayer, R.; Müller, I.; Müller, C. E. *Drug Dev. Res.* **2003**, *59*, 72–82.
51. Tripoli, E.; La Guardia, M.; Giammanco, S.; Di Majo, D.; Giammanco, M. *Food Chem.* **2007**, *104*, 466–479.
52. Mayer, R. *Phytochemistry* **1990**, *29*, 1340–1342.
53. Mayer, R. *Planta Med.* **1993**, *59*, 269–271.
54. Mayer, R. *J. Nat. Prod.* **1999**, *62*, 1274–1278.
55. Mayer, R. *Phytochemistry* **2004**, *65*, 593–601.
56. Manthey, J. A.; Guthrie, N.; Grohmann, K. *Curr. Med. Chem.* **2001**, *8*, 135–153.
57. Merino, G.; Jonker, J. W.; Wagenaar, E.; van Heraarden, A. E.; Schinkel, A. H. *Mol. Pharmacol.* **2005**, *67*, 1758–1764.
58. Haenisch, B.; Gilsbach, R.; Bönisch, H. *J. Neural. Trans.* **2008**, *115*, 973–982.
59. Pfaffl, M. W. *Nucleic Acids Res.* **2001**, *29*(9), e45.
60. ACD/Labs, version 5.09, ACD pK_a DB, Advanced Chemistry Development, Toronto ON, Canada.
61. SPSS, version 14, SPSS, Chicago, IL, USA.
62. SYBYL 6.9–7.3 versions; Tripos Inc., 1699 South Hanley Road, St. Louis, MO 63114-2917.